ELSEVIER

Materials Science and Engineering A299 (2001) 287–295

MATERIALS SCIENCE & ENGINEERING A

www.elsevier.com/locate/msea

Shear localization and recrystallization in dynamic deformation of 8090 Al–Li alloy

Y.B. Xu [a], W.L. Zhong [a], Y.J. Chen [b], L.T. Shen [c], Q. Liu [b], Y.L. Bai [c], M.A. Meyers [b,*]

[a] *State Key Laboratory for Fatigue and Fracture of Materials, Institute of Metals Research, Chinese Academy of Sciences, Shenyang 110015, People's Republic of China*

[b] *Department of Mechanical and Aerospace Engineering, University of California, San Diego, La Jolla, CA 92093-0411, USA*

[c] *Laboratory for Non-Linear Mechanics of Continuous Media, Institute of Mechanics, Chinese Academy of Sciences, Beijing 110080, People's Republic of China*

Received 24 May 2000

Abstract

The microstructural evolution in localized shear deformation was investigated in an 8090 Al–Li alloy by split Hopkinson pressure bar (strain rate of approximately 10^3 s^{-1}) at ambient temperature and 77 K. The alloy was tested in the peak-, over-, under-, and natural-aged conditions, that provide a wide range of microstructural parameters and mechanical properties. Two types of localized shear bands were distinguished by optical microscopy: the deformed shear band and the white-etching shear band. They form at different stages of deformation during localization. There are critical strains for the occurrence of deformed and white-etching localized shear deformation, at the imposed strain rate. Observations by transmission electron microscopy reveal that the white-etching bands contain fine equiaxed grains; it is proposed that they are the result of recrystallization occurring during localization. The deformed-type bands are observed after testing at 77 K in all heat treatment conditions, but they are not as well defined as those developed at ambient temperature. Cracking often occurs along the localized shear at ambient temperature. The decrement in temperature is favorable for the nucleation, growth and coalescence of the microcracks along the shear bands, inducing fracture.

Keywords: Shear localization; Recrystallization; Dynamic deformation; 8090 Al-Li alloy

1. Introduction

Shear localization is an important mode of deformation and occurs quite frequently in a variety of materials during dynamic loading. Recent investigations show that this mode of deformation sometimes also appears in single monotonic tensile[1–3] and cyclic fatigue[4] testing. Because of its technological importance it poses an interesting challenge to researchers. The formation, evolution and micromechanisms of localized shear deformation have received much attention in recent years, especially during the past two decades. Mechanicians have focused their efforts on the constitutive description, developing criteria for instability of plastic flow. Examples are the analyses of Recht [5], Culver [6], Clifton [7], Bai [8], Curran et al. [9], Burns and Trucano [10], Molinari and Clifton [11], and Wright [12]. Most of these approaches consist of a combination of a mechanical and thermal instability analysis. Materials scientists have emphasized the role of localized shear deformation in engineering applications, mainly the relationship between deformation-induced microstructures and residual mechanical properties (e.g. Bai and Dodd [13] and Meyers [14]). The complex interrelationships between stress, stress state, strain, strain rate and temperature, have been used for pursuing a better design of materials with the objective of postponing and even avoiding localized shear deformation [15–27].

This paper presents the results of an investigation on the formation and microstructural evolution of the

* Corresponding author. Tel.: +1-858-5344719; fax: +1-858-5345698.

E-mail address: mameyers@ucsd.edu (M.A. Meyers).

0921-5093/01/$ - see front matter
PII: S0921-5093(00)01412-X

shear localization produced during dynamic loading of an 8090 Al–Li alloy by split Hopkinson pressure bar at a strain rate of approximately 10^3 s^{-1} at both 298 and 77 K.

2. Materials and procedure

The alloy used in this investigation has the following nominal composition(wt.%): 2.5%Li, 1.11%Cu, 1.16%Mg, 0.16%Zr, and the balance Al. It was heat treated at peak-, over-, under- and natural-aged conditions, that provide a wide range of microstructural parameters and mechanical properties. The alloy bar was machined into cylindrical specimens 5 mm in diameter and 5 mm in height. The dynamic impact compression tests were performed in a modified split Hopkinson bar (Kolsky bar) at strain rates in the order of 10^3 s^{-1}. The applied stress was parallel to the rolling direction. The specimens after dynamic impact compression testing were characterized by optical, scanning, and transmission electron microscopy to establish the formation and microstructural evolution of localized shear deformation.

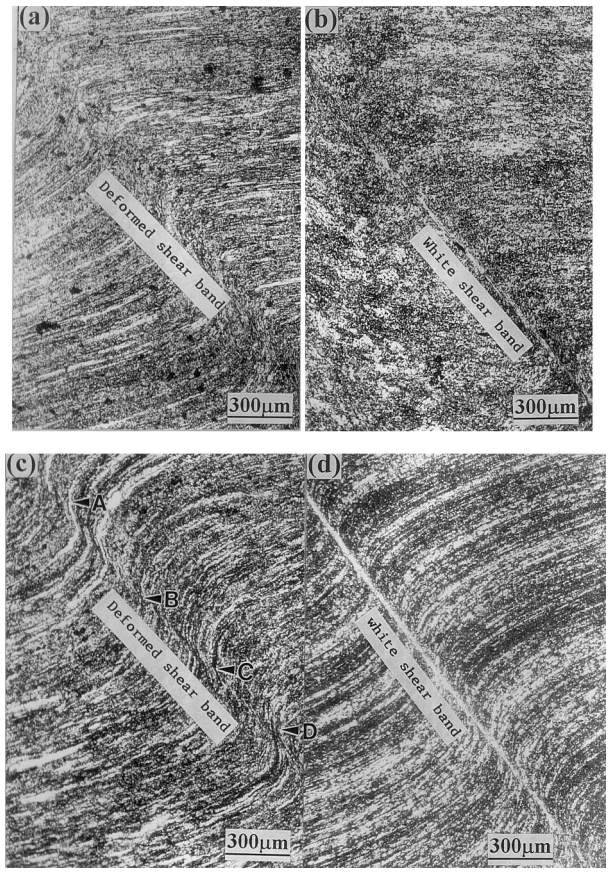

Fig. 1. Micrographs showing the deformed and white shear bands in peak-aged (a, b) and over-aged (c, d) alloy.

3. Results and discussion

3.1. Deformed and white-etching shear bands

Two types of localized shear bands were distinguished by optical microscopy for all four aged conditions. One is the deformed shear band, and the other the white shear band, as shown in Fig. 1a, c and b, d, respectively. The white shear band presented here is often referred to as the 'transformed shear band' or white-etching band in steels (Andrews et al. [28], McIntire and Manning [29], Manion and Stock [30], Thornton and Heiser [31], Woodward and Aghan [32], Rogers [15], Meyers and Wittman [33], Cho and Duffy [34], Zurek [35]), and in Ti-alloys (Timothy and Hutchings [36], Grebe et al. [37], Me-Bar and Shechtman [38]). TEM and X-ray diffraction led to the identification of these structures variously as quenched martensite, retained austenite, and delta ferrite. Meyers and Pak [39], Wittman et al. [40], and Beatty et al. [41] suggested that these 'transformed bands' were actually composed of submicron sized grains resulting from dynamic recrystallization: this will be discussed further in Section 3.5. On the basis of these experimental results, it is likely that the microstructure in the shear band is not unique and depends on the original structure of the material and deformation history.

The deformed and white shear bands occur at different stages of deformation during localization. The deformed shear band occurs as a first stage of localization, and the white shear band is a consequence of further development of the deformed shear band. The white shear bands, in addition to etching behavior, have distinct boundaries and a well-defined width.

3.2. Critical strain for the occurrence of localization

The experiments reveal that there is a critical value of the strain (at a certain strain rate) for the occurrence of the deformed and white-etching shear bands in all four aging conditions of the 8090 Al–Li alloys. Fig. 2 shows the stress–strain curves for peak-aged 8090 Al–Li alloy. The results of four tests are shown. The initiation of deformed shear band occurs when the strain reaches 0.14 at the strain rate of 1600 s^{-1} as shown in Table 1.

After this value, with increasing strain, the localized shear deformation becomes more apparent, and the width of the band decreases. As the strain increases from 0.14 to 0.17, the white shear band appears. As can be seen in Table 1 the situation is the same for the under-aged 8090 Al–Li alloy. The existence of a critical strain for localization has been shown by Marchand and Duffy [42] and is predicted by the mechanical analyses [5–12]. In the simplest form the onset of localization should occur beyond the maximum of the stress in the adiabatic stress–strain curve ($d\sigma/d\varepsilon = O$).

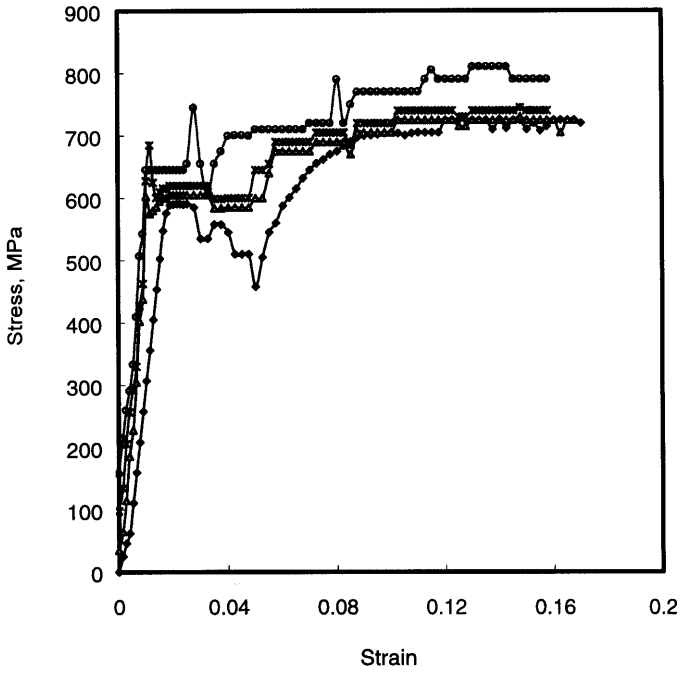

Fig. 2. Stress vs. strain response for the peak-aged Al–Li alloy.

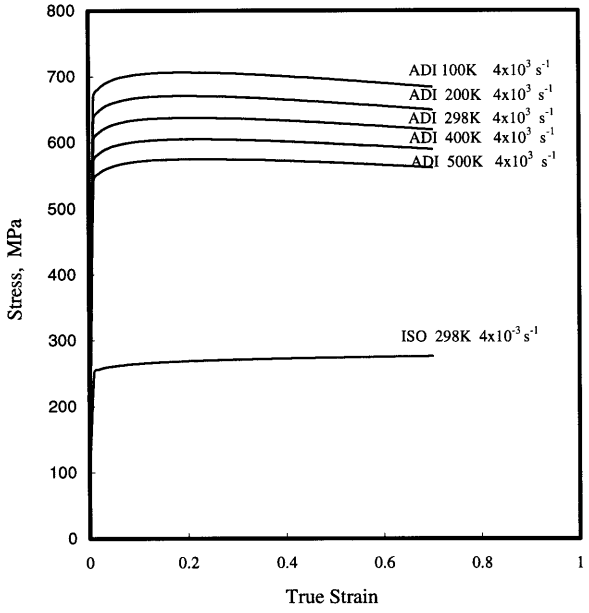

Fig. 3. Predicted stress vs. strain curves for Al–Li alloy in peak-aged condition based on the fitted Zerilli–Armstrong equation (ISO, isothermal; ADI, adiabatic).

Table 1
Critical strain for the occurrence of the localized shear band for peak-, and under-aged Al–Li alloys

	Peak-aged condition	Under-aged condition
Strain rate (s^{-1})	1600	2000
Critical strain for deformed band	0.14	0.17
Critical strain for white band	0.17	0.21

The Zerilli–Armstrong [43] equation was used to predict the mechanical response of the material. The parameters for the Zerilli–Armstrong equation are taken from a similar alloy (Al-3.2wt.%Li, Hines [44]). She carried out dynamic experiments at 77, 298, 323, and 423 K. Her Zerilli–Armstrong parameters and are given in Table 2.

$$\sigma = C_0 + C_2\varepsilon^n \exp(-C_3T + C_4T \ln \varepsilon) \quad (1)$$

The term C_0 was modified from the one used by Hines [44] in order to better fit the current experimental results.

The predicted stress–strain curves are shown in Fig. 3. For 4×10^3 s^{-1}, an adiabatic response is assumed. For 4×10^{-3} s^{-1}, an isothermal response is taken. The slight work hardening exhibited by the quasi-static curve contrasts with the softening response shown by the adiabatic curves in Fig. 3. The ambient temperature dynamic curve predicted from Zerilli–Armstrong is fairly close to the experimental results shown in Fig. 2. It is felt that this constitutive description of the mechanical response is satisfactory. It can also be seen that the maximum in the curve occurs for a plastic strain of approximately 0.2, in agreement with the observed strain for the initiation of deformed bands. This strain is not very sensitive to temperature. This instability strain is plotted as a function of initial deformation temperature in Fig. 4. Fig. 4 also shows the strain at which 0.5 T_m is reached (see calculation in Section 3.5). If we consider that 'white' shear bands are produced by dynamic recrystallization, then it becomes increasingly more difficult to generate them as the test temperature is lowered. The initiation of white-etching bands will be further discussed in Section 3.5.

Table 2
Zerilli–Armstrong parameters for Al–3.2 wt.%Li alloy (from Hines [44])

	C_0 (MPa)	C_2 (MPa)	C_3 (K^{-1})	C_4 (K^{-1} s^{-1})	n	δ
Al–Li alloy	80 (current) 40 (Hines[44])	720	0.0023	0.00016	0.03	0.014

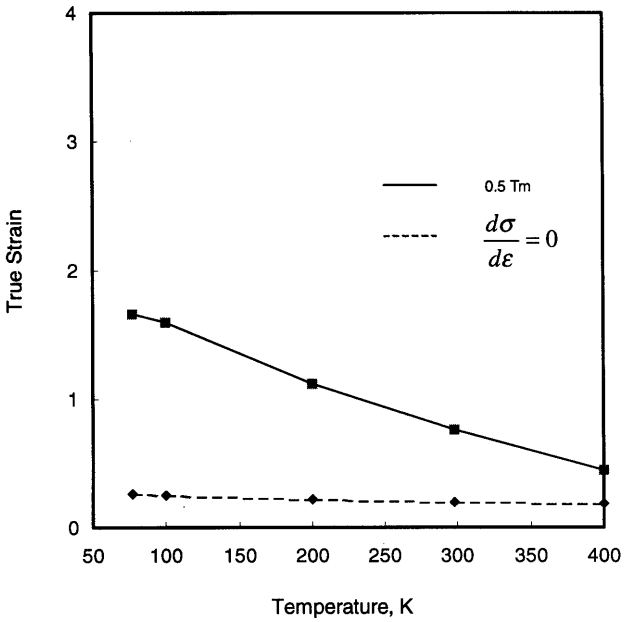

Fig. 4. Strains at onset of instability ($d\sigma/d\varepsilon$) and at $T_m/2$ (temperature equal to one half the melting point), as a function of initial temperature of test.

Table 3
Evolution of the localization for under-aged Al–Li alloy

Loading time (μs)	Width of the band (μm)	Average strain	Local strain
40	–	0.10	–
80	400	0.17	0.75
100	200	0.22	3.0
120	25	0.28	8.0

3.3. Material strength and localization

Low strain hardening rate, low specific heat, and high thermal softening increase the propensity for shear localization. Direct quantitative correlation between the critical strain for localized shear band formation and the strain-hardening coefficient has been obtained by Staker [45]; Dormeval and Ansart [46] found this relationship in martensitic steel. Table 3 gives the variation of the width, local strain and average strain of the localized shear band with the strength of the alloys. These results are also shown in Fig. 5. The average width of the band for peak-aged alloy with high strength and low strain-hardening capability is about 10 μm. However, for the natural aged Al–Li alloy, with low strength and high work-hardening capability, its average width is about 30 μm. The widths of the over- and under-aged Al–Li alloys are intermediate between these values. It should be mentioned that although the exact boundary of the band is not well defined, these values in are good agreement with the results obtained in Ti alloy [21] and in steel [24].

3.4. Evolution and propagation of localization

It is interesting to note that localized shear deformation is a gradually developing process with a certain velocity of propagation. The measurements show that the width and the local strain in the shear band varies along the shear direction. It can be seen clearly from Fig. 6 that the width of the band on the left part, marked by A, is about 20 μm, corresponding to a local strain of 5; in the middle part of the band, marked by B, the width is equal to approximately 30 μm with a local strain of 3. It can be seen that the shear band does not have well-defined boundaries at the tip (marked D). It is reasonable to propose that localization is a gradual propagation process along the shear direction, advancing with a characteristic velocity, as the loading time increases. The velocity of propagation can be roughly established by the length of the band (measured on the cross-section of the specimen), and the time required for the localization. The length of the band is about 6 mm, and the time required for localization is roughly 100 μs. Therefore, the velocity of the band propagation is established to be about 60 m s^{-1}. Zhou et al. [47]

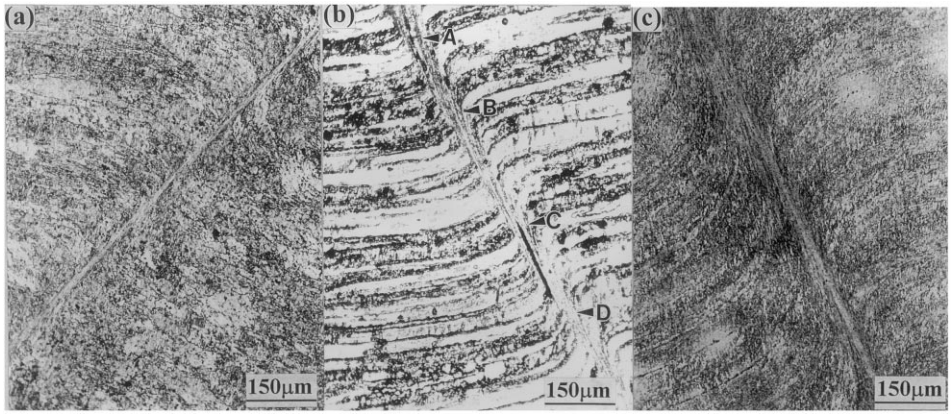

Fig. 5. Localized shear bands occurring in (a) peak-, (b) over-, and (c) natural-aged Al–Li alloy.

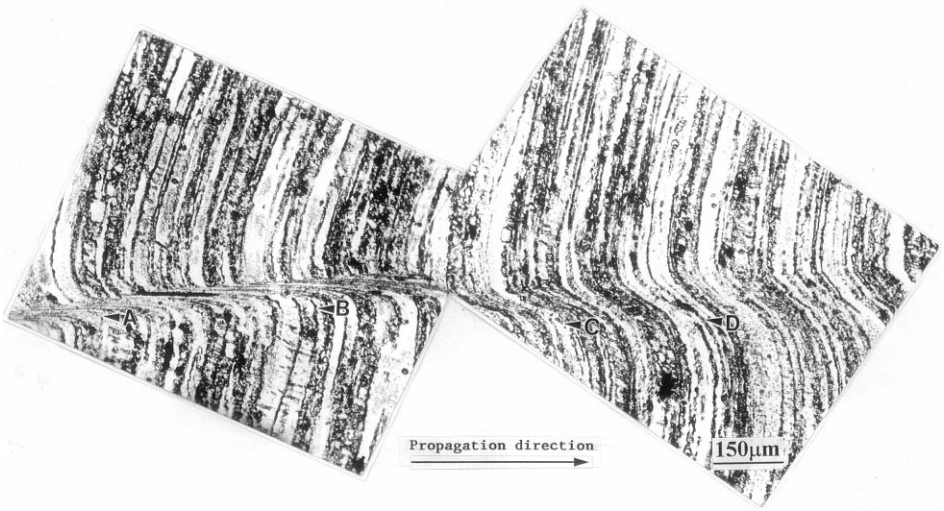

Fig. 6. Propagation of localized shear towards the shear direction.

have measured velocities of 50–75 m s^{-1} for an impact velocity of 64.5 m s^{-1} in Ti–6Al–4V alloy. This is fairly consistent with the current results.

A series of interrupted tests were performed on the modified SHPB at average strain rates of about 2250 s^{-1}, in order to characterize the evolution of localization. It is found that when the average strain is approximately 0.10, corresponding to a loading time of 40 μs, the deformation appears to be homogeneous, and there is no shear localization to be recognized in the cross-section. This is shown in Fig. 7a, implying that the specimen tested is still work hardening. However, as the average strain increases from 0.10 to 0.17, corresponding to a loading time of 80 μs, shear localization with a local strain of 0.75 occurs, as shown in Fig. 7b. Beyond this point, the specimen appears to work soften, and with the increase in the loading time, the localization becomes more apparent as shown in Fig. 7c. When the loading time is about 120 μs, the shear band narrows, with a width of 25 μm and local strain of 8, as shown in Fig. 7d. Thus, the evolution of deformation is a rapid progressive process during which the localization becomes more apparent, and the width of the band becomes gradually narrower.

Dynamic compression tests have also been performed for all four heat treatment conditions at 77 K. Predictably, the experiments reveal that localized shear deformation is also observed, as shown in Fig. 8a. The shear bands are not so well developed, and the decrement in temperature is favorable for microcrack nucleation, growth and coalescence. The cracks propagate more easily at lower temperatures than at room temperature, inducing the fracture of the material as shown in Fig. 8b.

3.5. Recrystallization

The microstructure of the localized shear band was characterized by transmission electron microscopy. Fig. 9 shows TEM micrographs of the localized shear bands occurring in over-aged aged 8090 Al–Li alloy tested at ambient temperature. It can be recognized that the base alloy shows the deformed cell structure with a significant density of dislocations (Fig. 9a), and the region adjacent to the localized shear band is characterized by the elongated cells with well defined boundaries as shown in Fig. 9b. However, near the shear band, these elongated cells break drown, and the structure in the central region of the band consists of very fine equiaxed

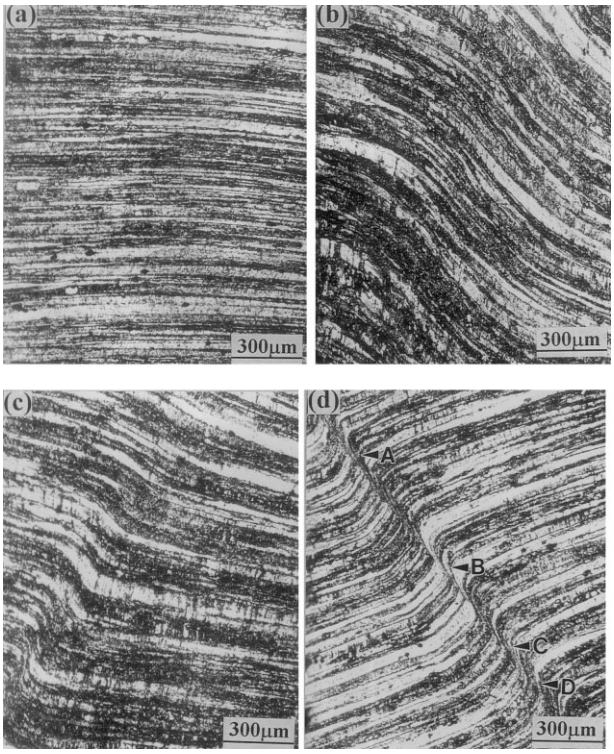

Fig. 7. Evolution of localized shear as strain is increased.

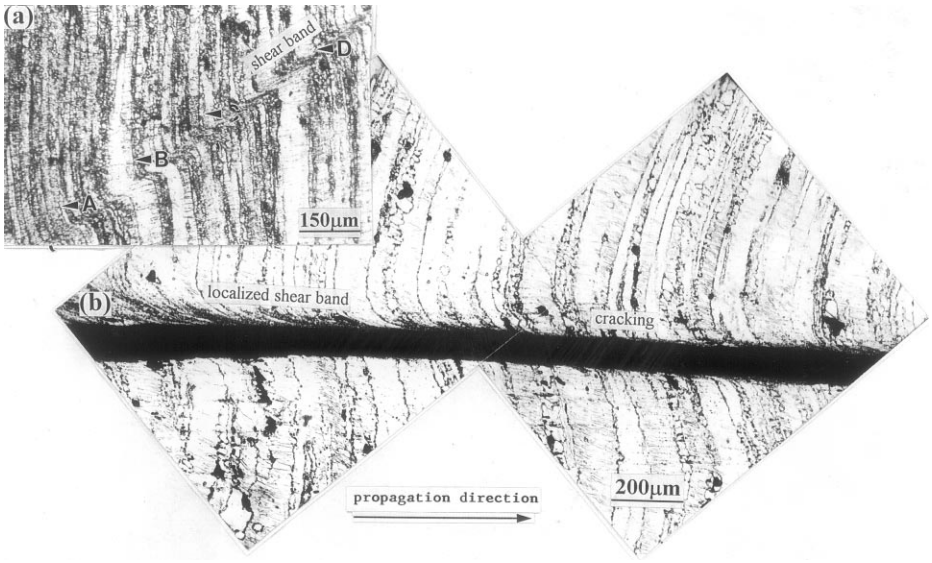

Fig. 8. (a) Localized shear deformation and (b) associated cracking along shear band occurring for initial deformation temperature of 77 K.

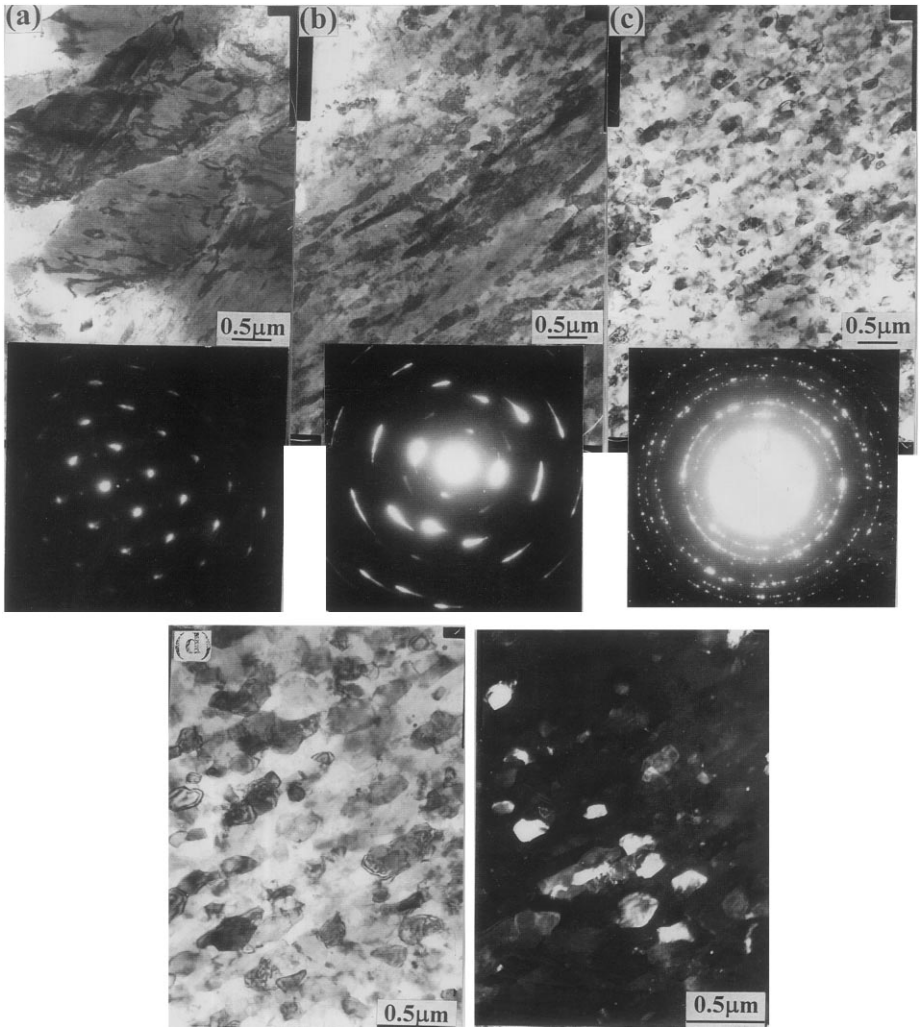

Fig. 9. TEM micrographs showing (a) the deformed structure in region of homogeneous deformation, (b) elongated cells adjacent to the band, and (c, d) recrystallized equiaxed grains with approximately 0.2 μm diameter within band.

grains with an average grain size of about 0.2 μm, and very low density of dislocations as shown in Fig. 9c. Fig. 9d shows the magnified bright and dark field images of Fig. 9c. It is clear that these small equiaxed grains have well defined boundaries, and the diffraction patterns arising from the band show that there is a nearly continuous ring of orientations on which there are distributed discontinuous spots. The absence of precipitates is indicative of a temperature excursion that exceeded the solvus line, which, for this alloy, is approximately 500°C. Coincidentally, this also corresponds to the recrystallization temperature. This evolution of the microstructure is reasonably explained by dynamic recrystallization, which was first observed and correctly postulated by Meyers and Pak [39] in titanium, and later confirmed in copper [48–50] and in tantalum [51]. This dynamic recrystallization takes place by a rotational mechanism, in contrast with the one observed after low-strain-rate deformation, which occurs by a migrational mechanism. This rotational dynamic recrystallization is described in more detail by Meyers et al. [52] and Andrade et al. [48]. It has been modeled, in terms of dislocations, by Meyers et al. [53,54] and, in continuum plasticity terms, by Hines and Vecchio [55,56]. A kinetic analysis has recently been proposed by Li et al. [57].

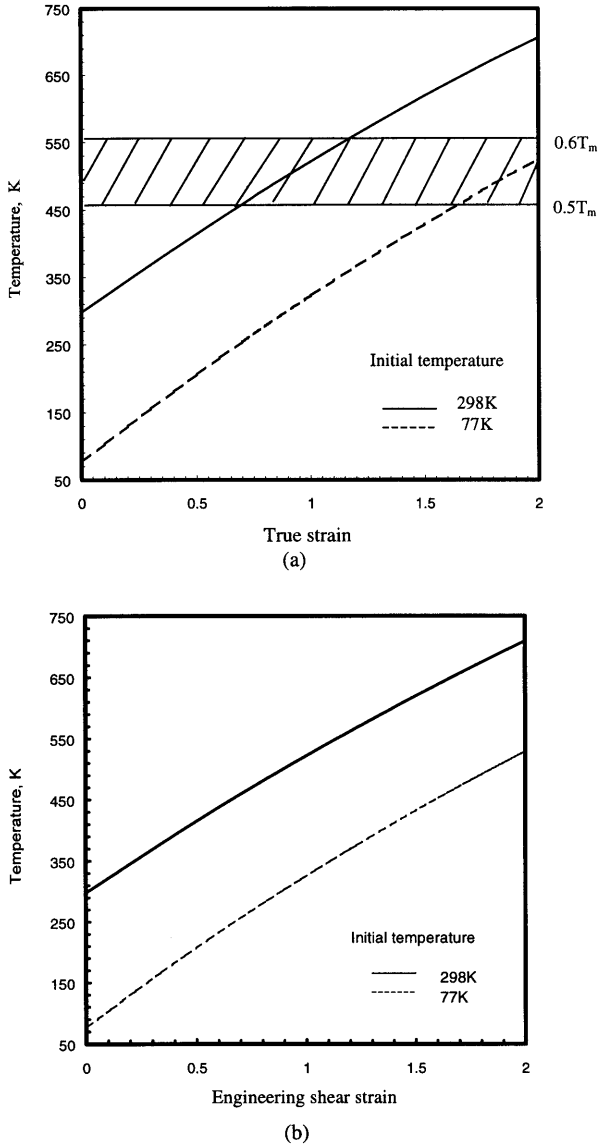

Fig. 10. Predicted temperature as a function of plastic strain for tests conducted at initial temperatures of 77 and 298 K; (a) temperature vs. true strain, ε; (b) temperature vs. engineering shear strain, γ.

It is becoming accepted that the large-strain deformation (in shear localization) occurring at high-strain-rate and the associated temperature rise can lead to a new recrystallized microstructure; however, it is not clear whether this recrystallized structure develops simultaneously with deformation (dynamic recrystallization) or subsequent to deformation (static recrystallization). This subject has been discussed in detail by Meyers et al. [53,54]. The temperature that produces thermal recovery or recrystallization process in metals is generally expressed by:

$$T = (0.4 \rightarrow 0.5)T_{\mathrm{m}}$$

The temperature rise was estimated by:

$$\mathrm{d}T = \frac{C_{\mathrm{p}}}{\beta\rho}\int \sigma \, \mathrm{d}\varepsilon \tag{2}$$

where ρ is the density and β is the work to heat conversion factor. β is taken as 0.9. The temperature dependency of the heat capacity, C_{p}, was considered. This is a significant effect at low temperatures. The following expression (for pure Al) was used:

$$C_{\mathrm{p}} = 20.108 + 1.32 \times 10^{-2}\ T + 3.3 \times 10^{4}\ T^{-2} \tag{3}$$

The predicted temperature rise is shown in Fig. 10a. It is obtained from Eqs. (1)–(3). The temperature excursion is shown for two initial temperatures: 77 and 298 K. The recrystallization temperature for Al–Li alloy can be safely taken as 0.5 T_{m} (T_{m} for Al is 933 K). In Fig. 10a a band is shown, bound by 0.5 and 0.6 T_{m}. It represents the recrystallization range. The true strain can be converted into an engineering shear strain through the expression:

$$\varepsilon = \ln \sqrt{1 + \gamma + \gamma^2} \tag{4}$$

Fig. 10b shows the temperature as a function of engineering shear strain. These results can be more easily correlated to the shear strains within the shear bands ($\gamma = \tan\theta$, where θ is the angular deflection within the shear localization regions). Two important conclusions can be derived from Fig. 10:

1. The strain at which localization leads to recrystallization is much lower for 298 K than for 77 K tests; the shear strains are approximately 0.67 and 1.59 for these two initial temperatures, respectively.

Table 4
Calculated shear strains (γ) for different experiments (position A, B, C, D marked in the Figures)

Figure number	A	B	C	D
1	5.7	8.4	9.6	14
5	1.2	2	1.9	2.9
6	1.2	1.8	2.4	2
7	7.3	12	15	12.9
8	4.5	2.7	2.9	4.6

2. For 77 K, fracture sets in prior to recrystallization. Fracture is a strain-governed phenomenon, and the critical strain for void/crack initiation precedes the temperature at which recrystallization occurs.

Table 4 shows the shear strain at various positions within shear bands. These shear strains are as high as 12. These strains were estimated by taking the angular deflection of the microstructural features that serve as fiducial marks. By comparing these values with the values in Fig. 10b, the temperature rises can be estimated. The recrystallization temperature (0.5 T_m) is reached for a shear strain of approximately 1. The strains in Table 4 exceed the recrystallization strains. Thus, dynamic recrystallization is a likely mechanism of structural recovery in the shear bands.

4. Conclusions

(1) Two types of localized shear bands were observed for the four heat treatment conditions of the 8090 Al–Li alloy: deformed shear bands and white-etching shear bands. (2) There are critical values of strain for the occurrence of the deformed shear band and white shear band. They form at different stages of deformation. The deformed shear band appears in the first stage of localization, and the white shear band is a result of further shear. (3) The localized shear bands are not well defined for specimens tested at 77 K; the decrement in temperature favors microcrack nucleation, growth and coalescence in the band, which lead to premature failure, before the shear bands develop. (4) Dynamic recrystallization is proposed to be the mechanism to explain the observed microstructure consisting of grains with diameters of approximately 0.2 μm.

Acknowledgements

This work was supported by National Nature Science Foundation of China No. 19891180-2 and by the US Army Research Office MURI Program (Contract DAAH 04-96-1-0376). Discussions with Professor K.S. Vecchio and Dr J.A. Hines are greatly appreciated.

References

[1] Y.B. Xu, Z.G. Wang, Z.Q. Hu, Metall. Trans. 22A (1991) 723.
[2] Y.B. Xu, E.A. Starke, Jr., R.P. Gangloff, Tensile deformation and fracture behavior of a rapidly solidified Al–Fe–V–Si alloy at ambient and elevated temperature, unpublished report (1992), Department of Materials Science and Engineering, University of Virginia.
[3] Y.B. Xu, Z.G. Wang, Z.Q. Hu, Scr. Metall. 5 (1991) 1149.
[4] S.S. Kim, M.J. Maynes, R.P. Gangloff, Mater. Sci. Eng. A203 (1995) 256.
[5] R.F. Recht, J. Appl. Mech. 31 (1964) 189.
[6] R.S. Culver, in: R.W. Rhode, B.M. Butcher, J.R. Holland, C.H. Karnes (Eds.), Metallurgical Effects at High Strain Rates, Plenum, New York, 1973, p. 519.
[7] R.J. Clifton, Material Response to Ultra-High-Loading-Rates, National Materials Advisory Board, N.A.S., Report NMAB 356, 1979, p. 129.
[8] Y.B. Bai, in: M.A. Meyers, L.E. Murr (Eds.), Shock-Wave and High-Strain-Rate Phenomena, Plenum, New York, 1981, p. 277.
[9] D.R. Curran et al., Computation model for armor phenomena, SRI International Report, 1979.
[10] T.J. Burns, T.G. Trucano, Mech. Mater. 1 (1982) 313.
[11] A. Molinari, R.J. Clifton, C.R. Acad. Sci. Paris 296 (1983) 1.
[12] T.W. Wright, J. Mech. Phys. Solids 35 (1987) 95.
[13] Y. Bai, B. Dodd, Adiabatic Shear Localization, Pergamon Press, Oxford, 1992.
[14] M.A. Meyers, Dynamic Behavior of Materials, Wiley, New York, 1994, p. 448.
[15] H.C. Rogers, Ann. Rev. Mater. Sci. 9 (1979) 283.
[16] R.L. Woodward, Metall. Trans. 10A (1979) 283.
[17] Y. Me-Bar, D. Shechtman, Mater. Sci. Eng. 58 (1983) 181.
[18] M.A. Meyers, C.L. Wittman, Metall. Trans. 21A (1990) 3153.
[19] J.H. Giovanola, Mech. Mater. 7 (1988) 73.
[20] K. Cho, Y.C. Chi, J. Duffy, Metall. Trans. 21A (1990) 1161.
[21] Y.L. Bai, Q. Xue, Y.B. Xu, L.T. Shen, Mech. Mater. 17 (1994) 155.
[22] M.A. Meyers, U.R. Andrade, A.H. Chokshi, Metall. Trans. 26A (1995) 2881.
[23] B. Dodd, A.G. Atkins, Acta Metall. 31 (1983) 9.
[24] Y.B. Xu, Y.L. Bai, Q. Xue, L.T. Shen, Acta Metall. Mater. 44 (1996) 1917.
[25] Y.B. Xu, Y.L. Bai, Mater. Sci. Eng. 114 (1989) 81.
[26] S. Pappu, S. Niou, C. Kennedy, L.E. Murr, Duplessis, M.A. Meyers, in: L.E. Murr, K.P. Staudhammer and M.A. Meyers (Eds.), Metallurgical and Materials Applications of Shock-Wave and High-Strain-Rate Phenomena, Elsevier, Amsterdam, 1995, p. 495.
[27] M.A. Meyers, V.F. Nesterenko, Y.J. Chen, J.C. LaSalvia, M.P. Bondar, Y.L. Lukyanov, in: L.E. Murr, K.P. Staudhammer, M.A. Meyers (Eds.), Metallurgical and Materials Applications of Shock-Wave and High-Strain-Rate Phenomena, Elsevier, Amsterdam, 1995, p. 487.
[28] J.H. Andrews, H. Lee, L. Bourne, D.V. Wilson, JISI 165 (1950) 369.
[29] H.O. McIntire, G.K. Manning, Met. Prog. 94 (1958).
[30] S.A. Manion, T.A.C. Stock, Int. J. Fract. Mech. 6 (1970) 106.
[31] P.A. Thornton, F.A. Heiser, Metall. Trans. 2A (1971) 1496.
[32] R.L. Woodward, R.L. Aghan, Met. Forum. 1 (1978) 180.
[33] M.A. Meyers, C.L. Wittman, Metall. Trans. 4321 (1990) 3153.
[34] K. Cho, Y.C. Chi, J. Duffy, Metall. Trans. 21A (1990) 1162.
[35] A.K. Zurek, Metall. Trans. 25A (1994) 2483.
[36] S.P. Timothy, I.M. Hutchings, Acta Metall. 33 (1985) 667.
[37] H.A. Grebe, H.-r. Pak, M.A. Meyers, Metall. Trans. 16A (1985) 761.
[38] Y. Me-Bar, D. Schechtman, Mater. Sci. Eng. 58 (1983) 181.

[39] M.A. Meyers, H.-R. Pak, Acta Metall. 34 (1986) 2493.
[40] C.L. Wittman, M.A. Meyers, H.-R. Pak, Metall. Trans. 21A (1990) 707.
[41] J.H. Beatty, L.W. Meyer, M.A. Meyers, S. Nemat-Nasser, in: M.A. Meyers, L.E. Murr, K.P. Staudhammer (Eds.), Shock Wave and High-Strain-Rate Phenomena in Materials, Marcel Dekker, New York, 1992, p. 645.
[42] A. Marchand, J. Duffy, J. Mech. Phys. Solids 36 (1988) 251.
[43] F.J. Zerilli, R.W. Armstrong, J. Appl. Phys. 61 (1987) 1816.
[44] J.A. Hines, Kinetics of recrystallization in adiabatic shear bands, PhD Thesis, University of California, San Diego, CA, 1996, p. 97.
[45] M.R. Staker, Acta Metall. 29 (1981) 683.
[46] R. Dormeval, J.P. Ansart, International Conference on Mechanical and Physical Behavior of Materials under Dynamic Loading (DYMAT 85), Editions de Physique, Paris, 1985, p. 299.
[47] M. Zhou, G. Ravichandran, A.J. Rosakis, J. Mech. Phys. Solids 44 (1996) 981 see also p. 1007.
[48] U. Andrade, M.A. Meyers, K.S. Vecchio, A.H. Chokshi, Acta Metall. Mater. 42 (1994) 3183.
[49] M.A. Meyers, U.R. Andrade, A.H. Chokshi, Metall. Trans. 26A (1995) 2881.
[50] J.A. Hines, K.S. Vecchio, Proc. 3rd Int. Conf. on Recrystallization and Related Phenomena (ReX'96), T. McNelley (Ed.), p. 179.
[51] M.A. Meyers, Y.J. Chen, F.D.S. Marquis, D.S. Kim, Metall. Trans. 26A (1995) 2493.
[52] M.A. Meyers, G. Subhash, B.K. Kad, L. Prasad, Mech. Mater. 17 (1994) 175.
[53] M.A. Meyers, J.C. LaSalvia, V.F. Nesterenko, Y.J. Chen, B.K. Kad, Proc. of 3rd Int. Conf. on Recrystallization and Related Phenomena (ReX'96), T. McNelley (Ed.), p. 279.
[54] M.A. Meyers, Q. Xue, V.F. Nesterenko, J.C. LaSalvia, Mater. Sci. Eng., (1999) (accepted).
[55] J.A. Hines, K.S. Vecchio, Acta Metall. Mater. 45 (1997) 635.
[56] J.A. Hines, K.S. Vecchio, S. Ahzi, Metall. Mater. Trans. 29 (1998) 191.
[57] Q. Li, Y.B. Xu, Z.H. Lai, L.T. Shen, Y.L. Bai, Mater. Sci. Eng. A276 (2000) 127.